Smart Structures and Systems, *Vol. 31*, *No. 1* (*2023*) *79-88*
https://doi.org/10.12989/sss.2023.31.1.079

Safety diagnosis process for deteriorated buildings using a 3D scan-based reverse engineering model

Jae-Min Lee [1a], Seungho Kim [2b] and Sangyong Kim*[1]

[1] *Department of Architecture*, *Yeungnam University*, *280 Daehak-ro*, *Gyeongsan-si*, *Gyeongsangbuk-do*, *Republic of Korea*
[2] *Department of Architecture*, *Yeungnam University College*, *170 Hyeonchung-ro*, *Nam-gu*, *Daegu*, *Republic of Korea*

(*Received September 28*, *2021*, *Revised May 23*, *2022*, *Accepted September 12*, *2022*)

Abstract. As the number of deteriorated buildings increases, the importance of safety diagnosis, maintenance, and the repair of buildings also increases. Traditionally, building condition assessments are performed by one person or one company and various inspections are needed. This entails a subjective judgment by the inspector, resulting in different assessment results, poor objectivity and a lack of reliability. Therefore, this study proposed a method to bring about accurate grading results of building conditions. The limitations of visual inspection and condition assessment processes previously conducted were identified by reviewing existing studies. Building defect data was collected using the reverse-engineered three-dimensional (3D) model. The accuracy of the results was verified by comparing them with the actual evaluation results. The results show a 50% time-saving to the same area with an accuracy of approximately 90%. Consequently, defect data with high objectivity and reliability were acquired by measuring the length, area, and width. In addition, the proposed method can improve the efficiency of the building diagnosis process.

Keywords: 3D point cloud; deterioration buildings; laser scanner; reverse engineered 3D model; unmanned aerial vehicle

1. Introduction

With the recent increase in the number of deteriorated buildings, the importance of building safety diagnosis and maintenance measures is increasing, and mid- to long-term management plans are necessary (Celik *et al*. 2018). To this end, relevant laws on building inspection, management, and repair have been established to maintain the performance of deteriorated buildings. The existing safety diagnosis process for status evaluation rating is based on visual inspections, and several inspections are generally conducted by one person or one company. This may introduce subjective judgment of inspectors, resulting in different evaluation results and poor reliability of the data (Park *et al*. 2017). In addition, any loss of documents incurs additional costs for rework. In contrast, precise safety diagnoses with expensive equipment are costly and time-consuming (Faqih *et al*. 2020). In exterior inspections of deteriorated buildings for status evaluation rating, efficiency is reduced by non-standardized processes and reporting systems (Kwan and Ng 2015, Shi and Ergan 2020).

To address these issues, several studies have recently addressed exterior inspections of deteriorated buildings using high-precision measuring devices (Jung *et al*. 2019, Liu *et al*. 2019, Falorca and Lanzinha 2020). However, although these studies enabled the collection of objective data, the determined status evaluation rating of buildings had poor accuracy. Moreover, previous studies are less reliable as errors in the exterior inspection data acquired through high-precision measuring devices were not verified. This study aims to analyze the exterior inspection methods in the existing safety diagnosis process of deteriorated buildings, as well as the reasons for the limitations of the safety diagnosis. Exterior inspection data were collected based on three-dimensional (3D) scans, and measures to improve the efficiency of the safety diagnosis were determined using a reverse engineering 3D model. First, based on the detailed guidelines for precision inspection and precision safety diagnosis provided by the Korea Authority of Land & Infrastructure Safety, the criteria and standards for exterior inspection evaluation, which serve as the standard for the safety diagnosis of deteriorated buildings, were identified. Second, a reverse engineering model developed with an unmanned aerial vehicle (UAV) and a laser scanner was used to determine the status evaluation rating of deterioration buildings. Finally, the accuracy of the data was verified by examining the differences between the data acquired through the 3D scan reverse engineering model and those acquired through visual inspection, and the effect of these errors on the status evaluation rating

*Corresponding author, Ph.D., Professor,
E-mail: sangyong@yu.ac.kr
[a] M.S., E-mail: jerry0719@ynu.ac.kr
[b] Professor, E-mail: kimseungho@ync.ac.kr

ISSN: 1738-1584 (Print), 1738-1991 (Online)

2. Review of previous studies

2.1 Limitations of previous studies

The deterioration of building exteriors has emerged as a serious public safety issue in modern society (Shi and Ergan 2018). Visual inspection is one of the conventional methods of exterior inspection by making visual measurements or using measuring devices according to detailed guidelines and evaluation criteria tables (IM-19-E6-007 2019, Anuar *et al*. 2019). Visual inspection is a major stage in surveying the basic data for building inspection and includes the following nine items: strength, crack, neutralization, scaling, spalling & delamination, water leak & efflorescence, rebar exposure, slope, and displacement deformation (Kwan and Ng 2015, Park *et al*. 2016).

A visual inspection entails the subjective nature of inspection experts or examiners. Therefore, exterior inspection data acquired through visual inspection may not serve as objective evaluation data (Fils *et al*. 2021). For this reason, previous studies have presented issues related to the objectivity and reliability of exterior inspection data acquired through visual inspection. Kwan and Ng (2015) stated that the existing exterior inspection process was not standardized, which would require additional time for rework, reduce the objectivity of the data, and consequently increase costs. Park *et al*. (2017) reported that private companies were primarily selected through the lowest bidding to perform safety diagnoses, and the exterior inspection results were less objective as they depended on the level and perspective of individual experts. According to Liu *et al*. (2019), in exterior inspection based on the existing safety diagnosis, a single expert evaluates each item on the checklist along the inspection route, which is very labor-intensive and time-consuming. Shi and Ergan (2020) suggested that the exterior inspection methods and practices should be analyzed by subdividing the work process, and that the external inspection methods and reporting formats should be standardized. In summary, the data acquired through the existing exterior inspection process are influenced by the differences in the level of knowledge and perspective of inspection experts, resulting in poor objectivity. The exterior inspection results are less reliable as they vary with the subjective nature of the inspectors. Moreover, an exterior inspection performed by a single expert is very labor-intensive, and the lack of standardized processes increases the amount of rework, time, and cost.

2.2 Status evaluation using high-precision measuring devices

With the recent development of high-precision devices with improved accuracy and the advancement of data mining techniques, more studies have been conducted on exterior inspection using UAVs to analyze the condition of buildings (Mondal and Jahanshahi 2020, Qi *et al*. 2021). Choi and Kim (2015) conducted a study to assess cracks and conditions by combining image processing technology with UAV technology. Falorca and Lanzinha (2020) identified the performance level of buildings and proposed maintenance measures by acquiring data through exterior inspection using UAVs and analyzing the preservation status of the External Thermal Insulation Composite System. Additionally, an increase in life expectancy was anticipated based on the comparison to the existing performance degradation curve and simple theoretical models.

Laser scanning technology is effective in creating geometric models of existing buildings or other structures (Huang *et al*. 2021). The mean error of data acquired with a laser scanner is approximately 2 mm to 3 mm for ordinary buildings, providing highly accurate 3D point cloud data (Vasić *et al*. 2014). In addition, 3D point cloud and stereo images acquired with a laser scanner have been studied over the past decade for crack detection and measurement, and have been proven to be capable of measuring fine cracks of 2 mm in size (Ani *et al*. 2015, Sarker *et al*. 2017). Law *et al*. (2015) confirmed that laser scanning technology provided very objective and precise data for exterior inspection and surface deterioration of buildings. Based on these studies, Turkan *et al*. (2018) analyzed 3D point cloud data to examine the damaged area of a tunnel, and studies were also conducted to identify cracks in damaged areas of large-scale structures, such as bridges and dams (Lattanzi and Miller 2014, Mukupa *et al*. 2016, Jang and An 2018, Zhang *et al*. 2019, Özcan and Özcan 2021). However, previous studies on 3D point cloud data acquired with UAVs and laser scanners were applied only to cracks, which is only one of the several items examined in the exterior inspection. Furthermore, the subjective nature is reflected in the process of drawing conclusions, which reduces objectivity, and the results are less reliable as they are not compared to actual values to verify accuracy. Moreover, previous studies focused on the status evaluation of large structures with relatively simple shape information, such as bridges and dams, requiring additional studies on buildings with complex shape information.

3. Reverse engineering modeling process

Reverse engineering is a process of identifying fundamental principles and operating systems through systematic analysis of devices, objects, and structures (Kim 2019). Reverse engineering technology is essential to perform exterior inspection and determine the status evaluation rating based on the shape information of the 3D point clouds of buildings. In addition, objective and accurate 3D point clouds should be acquired to determine the status evaluation rating using reverse engineering technology.

Reverse engineering technology can address the limitations related to the objectivity and reliability of data, as reported in previous studies, and also save time and costs, as status evaluation can be performed using only shape information without any special device. Therefore, in this study, a 3D model through reverse engineering was utilized with the shape information of buildings.

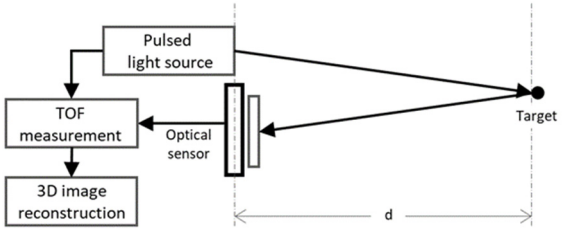

Fig. 1 Principles of laser scanning

3.1 Aquisition of 3D point cloud data based on high-precision measuring devices

In this study, image data were acquired through a UAV and laser scanner to extract 3D point cloud data. To record one specific object, image data must be acquired by setting the flight path of the UAV. Large-scale buildings are divided into sections, and the UAV path is set with overlapping sections. The acquired image data are used to extract 3D point cloud data with various software, such as Pix4D Mapper, ContextCapture, PhotoScan, and APS, and the reverse engineering 3D model can be constructed after an automatic alignment process.

Laser scanning refers to the methods and the applied technology for representing an exterior in a set of 3D point clouds by projecting a laser beam from the measuring device to an object at regular intervals and measuring the direction and distance of the reflected beam. The methods include the time-of-flight (T□F), triangulation, and shape-from-shades methods. In the T□F method, horizontal scanning is made possible by installing a measuring device on a rotational axis to rotate the device by a certain angle. Vertical scanning is performed by adjusting the laser reflection mirror inside the measuring device by a certain angle to acquire 3D point clouds for a wide range of objects (Fig. 1).

Therefore, 3D point clouds were acquired using the T□F method in this study. A 3D point cloud is a set of points containing thousands or millions of terrain data points with X, Y, and Z coordinates, and each of the data points is formed where the laser scanner is reflected from the object. The accuracy of the acquired 3D point cloud depends on the angle of the reflected laser beam and the reflectance of the surface of the object. In addition, there are areas where data cannot be acquired because the laser is projected radially, rather than in a straight line. Therefore, to obtain all exterior data, the building must be scanned by operating the laser scanner from at least two points. To acquire precise data, a large number of 3D point clouds should be acquired by increasing the number of shots, or the spacing of the 3D point cloud sets should be reduced. The 3D model constructed with the acquired 3D point clouds can provide shape information, which can be used to evaluate the building conditions, such as cracks, scaling, spalling, efflorescence, and rebar exposure.

3.2 3D point cloud registration process

1) Visual Alignment Registration

Visual alignment is a registration method in which the user manually registers 3D point clouds to the overlapping coordinates by aligning the scanning stations to the same coordinate plane space, followed by rotating and moving the data by the axis.

The process is as follows. The first image in Fig. 2(a) shows the preparation step for visual alignment by selecting two overlapping scanning stations. The second image in Fig. 2(a) shows the process of aligning the two scanning stations in the same coordinate plane space and overlapping them by moving the x and y axes. The third and fourth images in Fig. 2(a) show the process of moving the vertical displacement and overlapping the stations, respectively, because data may be acquired in areas where the ground is uneven after moving the horizontal displacement. The above process is repeated to complete a single reverse engineering 3D model.

2) Cloud to Cloud Registration

As it is difficult to acquire data for high floors and rooftops with a laser scanner, UAVs are used for these inaccessible locations. It is necessary to register the 3D models constructed with UAV data and with laser scan data. Thus, cloud-to-cloud registration was applied to register the two types of data. As shown in Fig. 2(b), the two completed ModelSpaces were selected, and the 3D models were rotated and moved such that they displayed the same feature. At least three features were subsequently selected, and the completed 3D model was verified after registration. For inaccurate registration, the previous process was repeated.

3) Noise Removal of Reverse Engineering 3D Model

Noise removal refers to eliminating unnecessary information, which is defined as “editing” in the program. The editing process is essential because it is difficult to run the completed model in other programs when it contains both the shape information of buildings and unnecessary information, resulting in an excessively large file size. Fig. 2(c) indicates the areas where the editing process was required, and Fig. 2(d) shows the reverse engineering 3D model after completing the editing process.

4. Case study

4.1 Data aquisition for status evaluation

A case study was conducted on a deteriorated building completed in 1976, with a floor area of 9,267.84 m^2 and three floors above the ground. External and internal data of the building were acquired using a laser scanner (BLK360, Leica geosystems, Inc.) with an accuracy of 6-8mm, and the data for the upper part of the building was acquired using an unmanned aerial vehicle (Inspire 2, DJI Co. Ltd). The 3D point cloud data acquired with the laser scanner and UAV were registered into a 3D model with shape information through the Cyclone program, and a reverse engineering 3D model was generated with the 3D Reshaper program. The total number of shots was 50 for the laser scanner and 231 for the UAV, and the total shooting time was 2 h 50 min. Additionally, 50 3D Point Cloud registration processes were

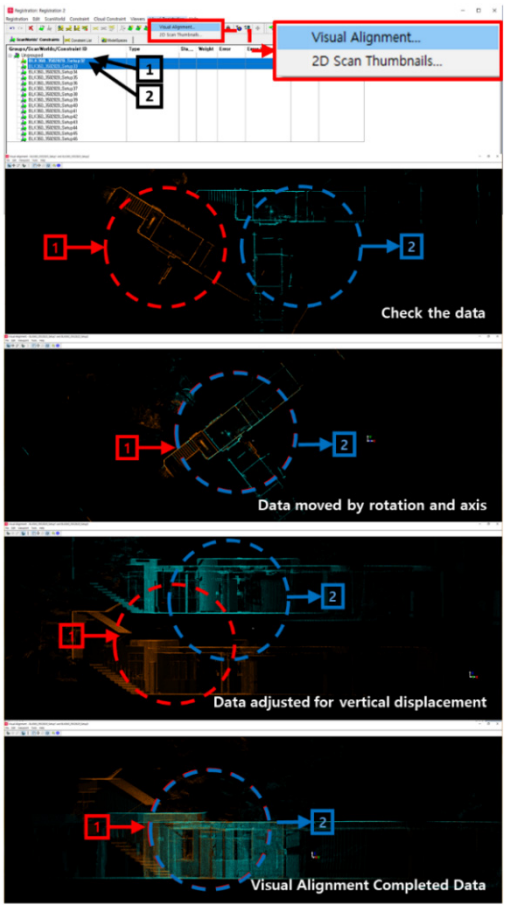

(a) Visual Alignment adjustment process

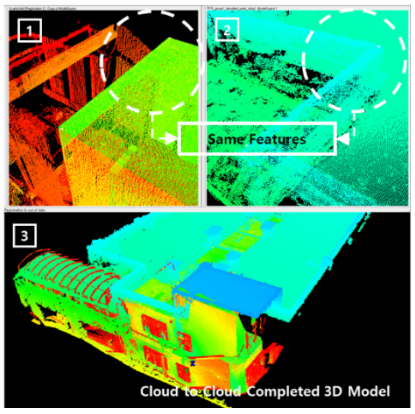

(b) Cloud to Cloud adjustment process

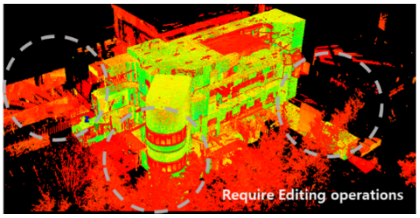

(c) Reverse Engineering 3D Models requiring Editing

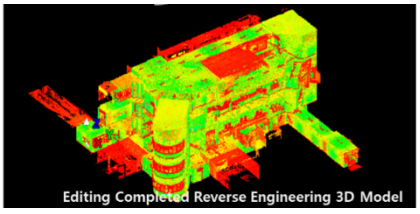

(d) Editing completed Reverse Engineering 3D Model

Fig. 2 3D point cloud adjustment process

obtained, which took 2 h 10 min, and the noise reduction and optimization process for Reverse Engineering 3D Modeling took 1 h. A condition assessment was then made on 55 points under seven evaluation criteria, which took 3 h and 10 min. As a result, the total time required for the process proposed in this study was 9 h 10 min, a decrease considering the 24 h required for visual inspection of the same area.

The visual inspection cost comprises the wages for one principal engineer ($30 per hour), one intermediate engineer ($22 per hour), and one junior engineer ($17 per hour). The estimated total cost is $1,656. This value is estimated based on South Korea's unit cost of wages. A total of $70 was calculated, including costs for one special technician ($30 per hour) and equipment rental ($40 per day) for the process proposed for this study. Consequently, the proposed process demonstrated high productivity and efficiency in time and cost.

4.2 Data measurement using 3D model

As the selected building is more than 30 years old, there are evaluation data available from the existing safety rating evaluation process. These data can be used to verify accuracy by comparing them to the data acquired through the status evaluation process proposed in this study for the 7 evaluation items and 55 locations (Fig. 3). This process was identified during the inspector's Reverse Engineering 3D Model visual inspection, and the width, depth, length, and area were measured using Reverse Engineering 3D Model. This process is depicted in Fig. 4. The extracted data values were compared with those obtained using the conventional visual inspection technique to verify the proposed method.

Deterioration data were collected using the completed reverse engineering 3D model for 7 items: cracks (31 locations), scaling (5 locations), spalling & delamination (3 locations), leaks & efflorescence (5 locations), rebar exposure (4 locations), slope (7 locations), and displacement deformation. The evaluation items and criteria stipulated by the Korea Authority of Land & Infrastructure Safety were adopted (Table 1).

1) Cracks

Fig. 4(a) shows the measurement for the cracks observed in the generated 3D model. The distance between the two endpoints over the width of the cracks was measured and analyzed considering the evaluation criteria stipulated by the Korea Authority of Land & Infrastructure Safety to determine the results. The comparative analysis of the actual and measured values of the 31 cracks indicated

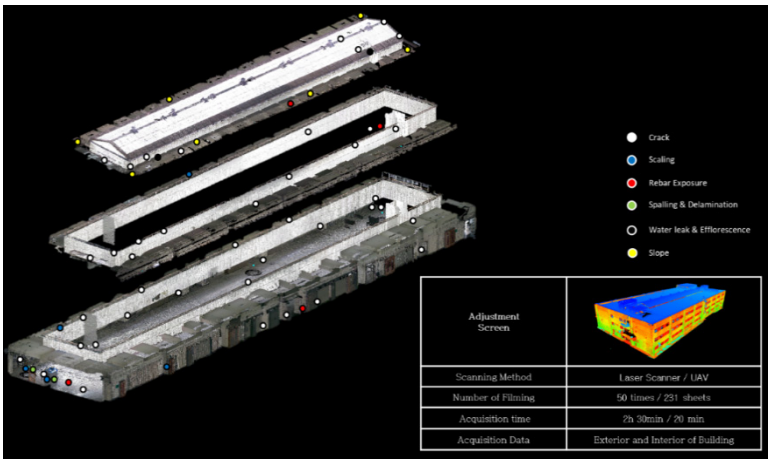

Fig. 3 Status assessment data measurement location

a mean error of 0.116 mm, and there was no change in the rating due to the error for 28 out of 31 cracks.

2) Scaling

Fig. 4(b) shows the results derived for concrete scaling. The depth values for scaling were derived by identifying and comparing the x, y, and z values of the points specified

Table 1 Status assessment criteria

	Rating	Score	Criteria		
			Maximum crack width : cw	Area Ratio : 20% or less	Area Ratio : 20% or more
Cracks	A	1	cw < 0.1	A	A
	B	3	0.1 ≤ cw < 0.2	B	C
	C	5	0.2 ≤ cw < 0.3	C	D
	D	7	0.3 ≤ cw < 0.5	D	E
	E	9	0.5 ≤ cw	E	E
	Rating	Score	Criteria		
			Scaling depth : sc	Area Ratio : 10% or less	Area Ratio : 10% or more
Scaling	A	1	sc = 0	A	A
	B	3	0 < sc < 0.5	B	B
	C	5	0.5 ≤ sc < 1.0	C	C
	D	7	1.0 ≤ sc < 25	D	D
	E	9	25 ≤ sc	E	E
	Rating	Score	Criteria		
			Spaling and delamination depth : sd	Area Ratio : 20% or less	Area Ratio : 20% or more
Spalling & delamination	A	1	sd = 0	A	A
	B	3	0 < sd < 15	B	C
	C	5	15 ≤ sd < 20	C	D
	D	7	20 ≤ sd < 25	D	E
	E	9	25 ≤ sd	E	E
	Rating	Score	Criteria		
Water leak & efflorescence	A	1	No water leak and efflorescence		
	B	3	If there is a trace of minor leakage in a dry state, or the area rate of whitening occurs is less than 5%		
	C	5	Significant signs of water leakage in wet conditions or less than 5% to 10% of white coating occurrence area		
	D	7	The progress of the leak is observable, or the area rate of whitening is less than 10-20%		
	E	9	The progress of leakage is evident, or the area rate of whitening occurs at least 20%		

Table 1 Continued

	Rating	Score	Criteria		
			Maximum crack width : cw	Area Ratio : 20% or less	Area Ratio : 20% or more
Rebar exposure	Rating	Score	Criteria		
	A	1	ra = 0		
	B	3	0 < ra < 1.0%		
	C	5	1.0 <= ra < 3.0		
	D	7	3.0 <= ra < 5.0		
	E	9	5.0 <= ra		
Displacement deformation	Rating	Score	Criteria		
	A	1	L (span length) / 480 or less		
	B	3	L / 480 or less		
	C	5	L / 240 or less		
	D	7	L / 150 or less		
	E	9	L / 150 or more		
Slope	Rating	Score	Criteria		
			Slope	Evaluation contents	
	A	1	1/750 or less	Risk subsidence limits on sensitive mechanical foundations.	
	B	3	1/500 or less	Construction Crack ccurrence Limits	
	C	5	1/250 or less	Detect the slope of a structure	
	D	7	1/150 or less	Limits to which structural damage is expected	
	E	9	1/150 or more	To the extent that the structure is dangerous	

in the scaled and normal concrete. The derived values and surface ratios were substituted into the stipulated evaluation criteria to determine the measured values. The mean error between the measured and actual values in 5 locations was minimal at 0.0246 mm, and there was no change in the rating for all 5 locations.

3) Spalling & delamination

Fig. 4(c) shows the results derived for concrete spalling and delamination. In the case of the selected building, the length of spalling corresponds to the depth, as the spalled area was located at the end of the eaves. Hence, the distance between the upper point of the spalled area and the lower point of the normal concrete, which corresponds to the spalling depth, was measured. The mean error between the measured and actual values in 3 locations was 0.86 mm, and there was no change in the rating due to the error.

4) Rebar exposure

Fig. 4(d) shows the measurement of the rebar exposure observed on the base side of the stairs. The status rating for rebar exposure was determined in terms of the area of the building. Based on the evaluation criteria, the error between the measured and actual values in 4 locations was 0.0028 m^2, and there was no change in the rating for the 4 locations.

5) Leaks & efflorescence

Fig. 4(e) shows the measurement of concrete leaks & efflorescence, and the status rating was determined based on the area of the building. The boundary of the area was specified by a polyline, and a mesh was created to calculate the area, which was used for the measurement of leaks & efflorescence. Subsequently, errors were determined through comparative analysis of the values measured according to the evaluation criteria and the actual values. The mean error between the measured and actual values in 5 locations was 0.0998 m^2 with no impact on the rating values.

6) Slope

Fig. 4(f) shows the slope measurement of the major straight member. The status evaluation of the slope was based on angular displacement. The mean error between the actual and measured values in 7 locations was minimal at 0.0001603 with no impact on the rating values.

7) Displacement deformation

Fig. 4(g) shows the measurement of concrete displacement deformation on the beam and slab structures. However, as no defects caused by differential settlement were observed during the exterior inspection of the building, the status for displacement deformation was considered to be stable and rated as “A”. Thus, comparison of actual and measured values was not possible. Data for seven criteria, comprising crack (thirty-eight points), scaling (two points), spalling & delamination (two points), leaks & efflorescence (three points), rebar exposure (four points), and slope (seven points) were collected based on the conventional visual inspection results. However, degradation data for the following seven criteria, consisting of crack (thirty-one points), scaling (five points), spalling &

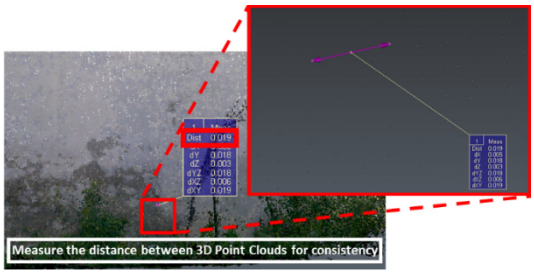

(a) Acquire results for concrete cracks

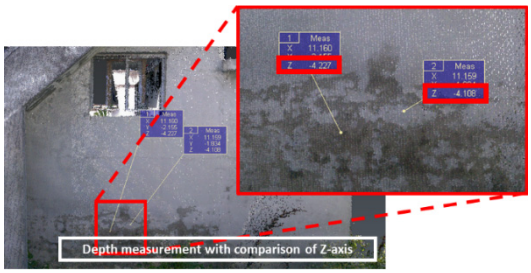

(b) Acquire results for concrete scaling

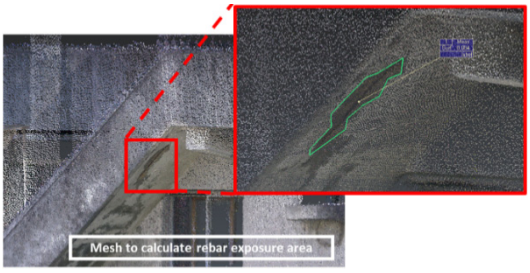

(c) Acquire results for concrete spalling & delamination

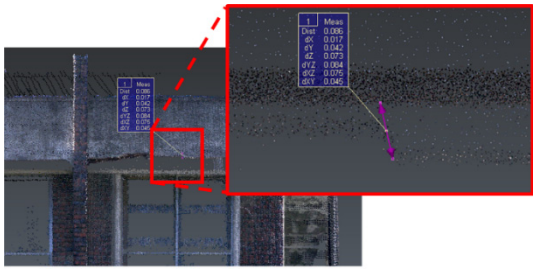

(d) Acquire results for rebar exposure

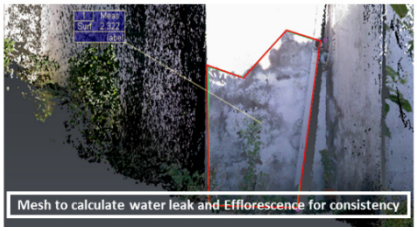

(e) Acquire of results for concrete water leak & efflorescence

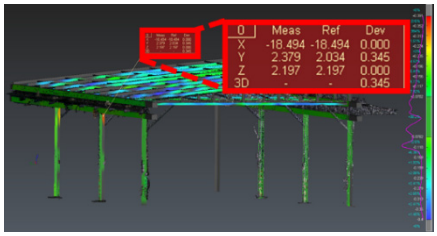

(f) Acquire Result for slope

(g) Acquire results for displacement deformation

Fig. 4 Reverse engineering 3D model-based condition assessment data acquisition process

delamination (three points), leaks & efflorescence (five points), rebar exposure (four points), and slope (seven points) were collected based on the building condition evaluation process proposed in this study. Data showing a decrease of seven points were collected for the crack criteria, and data showing increases of three points in scaling, one in spalling & delamination and two in leaks & efflorescence, were collected. This is attributed to the inability of the laser scanner to detect microcracks, owing to its accuracy and resolution limitations. □ther criteria showed an identical or increased data collection compared to the visual inspection results.

Table 2 presents a comparison and analysis of the error rate between the "measurement" performed in the building condition evaluation process and the "actual value" obtained through the conventional visual inspection proposed in this study. The "actual value" is the visual inspection value, which is the value obtained on-site using a crack microscope and a five-meter measuring tape. The result analysis confirmed a negligible error compared to the actual value. Although the crack category exhibited an error rate of 9%, this error was sufficiently small not to affect the status evaluation rating in the safety diagnosis of the deteriorated building, and the overall accuracy was found to be high.

5. Conclusions

In the safety diagnosis of buildings, it is important to acquire objective and reliable data for status evaluation. In this study, the existing safety diagnosis process was reviewed, and the limitations of poor objectivity and reliability due to the subjective nature of examiners were identified. To address these issues, a study was conducted on the acquisition method for 3D point cloud data and the improvement of objectivity in the acquired data.

To compare errors in the 3D point cloud data, visual inspection was performed on a three-story deteriorated building, and the corresponding data were compared to that obtained using the reverse engineering 3D model. The following items were evaluated: cracks, scaling, spalling & delamination, leaks & efflorescence, rebar exposure, and slope. The mean errors determined comparing the actual values of the target building in the case study and those obtained using the reverse engineering 3D model were: 0.116 mm for cracks, 0.0246 mm for scaling, 0.86 mm for spalling, 0.0998 m^2 for leaks & efflorescence, 0.0028 m^2 for rebar exposure, and 0.0001603 for slope.

As a result of the final review, minimal errors were observed for each item, which were sufficiently small not to affect the status evaluation rating in the safety diagnosis of deterioration buildings. In addition, the derived results exhibited a more conservative nature than the visual

Table 2 Error in acquired state evaluation data values

Classification	Actual value	Measurements	Error	State assessment	Accuracy
Crack (mm)	0.1	0.14	0.04	No change (A)	91%
	0.3	0.28	0.02	No change (C)	
	0.2	0.14	0.06	No change (B)	
	0.2	0.16	0.04	No change (B)	
	0.3	0.028	0.002	No change (C)	
	0.3	0.027	0.003	No change (C)	
	0.3	0.3	0	No change (C)	
	0.1	0.08	0.02	No change (A)	
	0.3	0.212	0.08	No change (C)	
	0.3	0.298	0.002	No change (C)	
	0.3	0.234	0.066	No change (C)	
	0.3	0.36	0.06	Change (C → D)	
	0.3	0.3	0	No change (C)	
	0.3	0.36	0.06	Change (C → D)	
	0.5	0.502	0.002	No change (E)	
	0.1	0.17	0.07	Change (A → B)	
	0.5	0.51	0.01	No change (E)	
	0.2	0.15	0.05	No change (B)	
	0.3	0.28	0.02	No change (C)	
	0.3	0.27	0.03	No change (C)	
	0.5	0.55	0.05	No change (E)	
	0.2	0.17	0.03	No change (B)	
	0.3	0.29	0.01	No change (C)	
	0.1	0.07	0.03	No change (A)	
	0.1	0.1	0	No change (A)	
	0.1	0.08	0.02	No change (A)	
	0.1	0.05	0.05	No change (A)	
	0.1	0.13	0.03	No change (B)	
	0.3	0.29	0.01	No change (C)	
	0.3	0.28	0.02	No change (C)	
	0.3	0.293	0.007	No change (C)	
Scaling (mm)	0.1	0.077	0.023	No change (A)	100%
	0.4	0.42	0.02	No change (A)	
	0.2	0.23	0.03	No change (A)	
	0.1	0.08	0.02	No change (A)	
	0.3	0.27	0.03	No change (A)	
Spalling & Delamination (mm)	11	10	1	No change (B)	100%
	3	4	1	No change (B)	
	3.4	4	0.6	No change (B)	
Water leak & Efflorescence (m^2)	1.35	1.367	0.017	No change (B)	100%
	0.315	0.5	0.152	No change (B)	
	1.135	0.113	0.022	No change (B)	
	1.004	0.796	0.208	No change (B)	
	0.318	0.510	0.1	No change (B)	

Table 2 Continued

Classification	Actual value	Measurements	Error	State assessment	Accuracy
Rebar exposure (m^2)	0.008	0.11	0.003	No change (B)	100%
	0.01	0.008	0.002	No change (B)	
	0.0037	0.006	0.0023	No change (B)	
	0.014	0.018	0.004	No change (B)	
Slope	0.00133	0.00177	0.00044	No change (A)	100%
	0.000253	0.000241	0.000012	No change (A)	
	0.000633	0.000633	0	No change (A)	
	0.000316	0.00316	0	No change (A)	
	0.000410	0.000275	0.000135	No change (A)	
	0.00120	0.000984	0.000216	No change (A)	
	0.00410	0.00121	0.0008	No change (A)	

inspection results, which can improve the reliability of the safety evaluation of buildings. Therefore, the suggested status evaluation process for deteriorated buildings based on the reverse engineering 3D model was highly objective and reliable. Moreover, the total time required for the process proposed was 9 h, which was more productive in terms of time and cost compared to the visual inspection of the same area. Thus, the process proposed is expected to save time and costs by acquiring status evaluation data without various expensive equipment used for existing safety diagnoses. However, as the analysis in this study is limited to reinforced concrete structures, additional research is required for other structures, such as steel frames and masonry walls, and a status evaluation process that can be applied for buildings of various structures needs to be stablished.

Acknowledgments

This work was supported by the National Research Foundation of Korea (NRF) grant funded by the Korea government (MSIT) (No. 2020R1A2C1005263).

References

Ani, A.I.C., Johar, S., Tawil, N.M., Abd Razak, M.Z. and Hamzah, N. (2015), "Building information modeling (BIM)-based building condition assessment: A survey of water ponding defect on a flat roof", *Jurnal Teknologi*, **75**(9), 25-31. https://doi.org/10.11113/jt.v75.5222

Anuar, M.Z.T., Sarbini, N.N., Ibrahim, I.S., □sman, M.H., Ismail, M. and Khun, M.C. (2019), "A comparative of building condition assessment method used in Asia countries: A review", *IOP Conference Series*: *Mater*. *Sci*. *Eng*., **513**(1), 012029. https://doi.org/10.1088/1757-899X/513/1/012029

Celik, □., Terrell, T., Gul, M. and Catbas, F.N. (2018), "Sensor clustering technique for practical structural monitoring and maintenance", *Struct*. *Monitor*. *Maint*., *Int*. *J*., **5**(2), 273-295. https://doi.org/10.12989/smm.2018.5.2.273

Craig, G. (2021), "Issue : Commercial Drones", SAGE business researcher, pp. 1-15.

Choi, S.S. and Kim, E.K. (2015), "Design and implementation of ision-based structural safety inspection system using small unmanned aircraft", *Proceeding of the 2015 17th International Conference on Advanced Communication Technology*, New York, USA, July. https://doi.org/10.1109/ICACT.2015.7224924

Choi, J., Yeum, C.M., Dyke, S.J. and Jahanshahi, M.R. (2018), "Computer-aided approach for rapid post-event visual evaluation of a building façade", *Sensors*, **18**(9), 3017. https://doi.org/10.3390/s18093017

Falorca, J.F. and Lanzinha, J.C.G. (2020), "Facade inspections with drones–theoretical analysis and exploratory tests", *Int*. *J*. *Build*. *Pathol*. *Adaptat*., **39**(2), 235-258. https://doi.org/10.12989/smm.2021.8.3.257

Faqih, F., Zayed, T. and Soliman, E. (2020), "BIM Based Facility Condition Assessment", *Proceedings of International Conference on Civil Infrastructure and Construction*, pp. 162-171. http://dx.doi.org/10.29117/cic.2020.0022

Fils, P., Jang, S. and Sherpa, R. (2021), "Field implementation of low-cost RFID-based crack monitoring using machine learning", *Struct*. *Monitor*. *Maint*., *Int*. *J*., **8**(3), 257-278. https://doi.org/10.12989/smm.2021.8.3.257

Fröhlich, C. and Mettenleiter, M. (2004), "Terrestrial laser scanning—new perspectives in 3D surveying", *Int*. *Arch*. *Photogramm*. *Remote Sens*. *Spatial Inform*. *Sci*., **36**(Part 8), W2.

Huang, H., Zhang, C. and Hammad, A. (2021), "Effective Scanning Range Estimation for Using TLS in Construction Projects", *J*. *Constr*. *Eng*. *Manage*., **147**(9), 04021106. https://doi.org/10.1061/(ASCE)C□.1943- 7862.0002127

IM-19-E6-007 (2019), Detailed Guidelines for Implementation of Safety and Maintenance of Facilities (Safety Inspection and Diagnostics) Instructions, Korea Authority of Land & Infrastructure Safety; Jinju, Korea.

Jang, K. and An, Y.K. (2018), "Multiple crack evaluation on concrete using a line laser thermography scanning system", *Smart Struct*. *Syst*., *Int*. *J*., **22**(2), 201-207. https://doi.org/10.12989/sss.2018.22.2.201

Jung, H.J., Lee, J.H., Yoon, S. and Kim, I.H. (2019), "Bridge Inspection and condition assessment using Unmanned Aerial Vehicles (UAVs): Major challenges and solutions from a practical perspective", *Smart Struct*. *Syst*., *Int*. *J*., **24**(5), 669-681. https://doi.org/10.12989/sss.2019.24.5.669

Kang, T.W., Kim, J.E. and Jung, T.S. (2016), "Deriving measures to improve MEP facility management work based on 3D reverse design", *JKAIS*, **17**(8), 38-45.

Kim, S.K. (2017), *Application and Utilization of Drone Imaging*, Korea Society Broadcasting Media Magazine, April.

Kim, S.H. (2019), "3D Point Cloud and 4D BIM-based Construction Project EV Tracking Process", Ph.D. Dissertation,

Yeungnam University, Gyeongsan, Korea.
Kwan, A.K.H. and Ng, P.L. (2015), "Building Diagnostic Techniques and Building Diagnosis: The Way Forward", *Engineering Asset Management-Systems*, *Professional Practices and Certification*, New York, USA. https://doi.org/10.1007/978-3-319-09507-3_74
Lattanzi, D. and Miller, G.R. (2014), "3D scene reconstruction for robotic bridge inspection", *J. Infrastr. Syst.*, **21**(2), 04014041. https://doi.org/10.1061/(ASCE)IS.1943-555X.0000229
Law, D.W., Holden, L. and Silcock, D. (2015), "The assessment of crack development in concrete using a terrestrial laser scanner (TLS)", *Austral. J. Civil Eng.*, **13**(1), 22-31. https://doi.org/10.1080/14488353.2015.1092635
Liu, D., Chen, J., Hu, D. and Zhang, Z. (2019), "Dynamic BIM-augmented UAV safety inspection for water diversion project", *Comput. Indust.*, **108**, 163-177. https://doi.org/10.1016/j.compind.2019.03.004
Liu, D., Xia, X., Chen. J. and Li, S. (2021), "Integrating building information model and augmented reality for drone-based building inspection", *J. Comput. Civil Eng.*, **35**(2), 04020073.
Mondal, T.G. and Jahanshahi, M.R. (2020), "Autonomous vision-based damage chronology for spatiotemporal condition assessment of civil infrastructure using unmanned aerial vehicle", *Smart Struct. Syst.*, *Int. J.*, **25**(6), 733-749. https://doi.org/10.12989/sss.2020.25.6.733
Mukupa, W., Roberts, G.W., Hancock, C.M. and Al-Manasir, K. (2016), "A review of the use of terrestrial laser scanning application for change detection and deformation monitoring of structures", *Survey Rev.*, **49**(353), 99-116. https://doi.org/10.1080/00396265.2015.1133039
Özcan, □. and Özcan, □. (2021), "Automated UAV based multi-hazard assessment system for bridges crossing seasonal rivers", *Smart Struct. Syst.*, *Int. J.*, **27**(1), 35-52. https://doi.org/10.12989/sss.2021.27.1.035
Park, H.J., Ryu, J.R., Woo, S.H. and Choo, S.Y. (2016), "Improvement of the Building Safety Inspection Survey Method using Laser Scanner and BIM-based Reverse Engineering", *J. Architect. Inst. Korea Plann. Des.*, **32**(12), 79-90. https://doi.org/10.5659/JAIK_PD.2016.32.12.79
Park, H.J., Lee, S.H., Kim, E.J. and Choo, S.Y. (2017), "A Proposal for Building Safety Diagnosis Processes Using BIM-Based Reverse Engineering Technology", *Proceeding of the 22nd International conference of the Association for Computer-Aided Architectural Design Research in Asia*, Hong Kong.
Qi, Y., Yuan, C., Kong, Q., Xiong, B. and Li, P. (2021), "A deep learning-based vision enhancement method for UAV assisted visual inspection of concrete cracks", *Smart Struct. Syst.*, *Int. J.*, **27**(6), 1031-1040. https://doi.org/10.12989/sss.2021.27.6.1031
Sarker, M.M., Ali, T.A., Abdelfatah, A., Yehia, S. and Elaksher, A. (2017), "A cost-effective method for crack detection and measurement on concrete surface", *Int. Arch. Photogramm. Remote Sens. Spatial Inform. Sci.*, **42**, 237. https://doi.org/10.5194/isprs-archives-XLII-2-W8-237-2017
Shi, Z. and Ergan, S. (2018), "Leveraging Point Cloud Data Detecting Building Facade Deteriorations Caused by Neighboring Consturction", *Tamap J. Eng.*, 2018. https://doi.org/10.29371/2018.3.66
Shi, Z. and Ergan, S. (2020), "Towards Point Cloud and Model-Based Urban Façade Inspection: Challenges in the Urban Façade Inspection Process", *Proceeding of the Constuction Research Congress 2020*: *Safety*, *Workforce*, *and Education*, Arizona, USA, March.
Turkan, Y., Hong, J., Laflamme, S. and Puri, N. (2018), "Adaptive wavelet neural network for terrestrial laser scanner-based crack detection", *Automat. Constr.*, **94**, 191-202. https://doi.org/10.1016/j.autcon.2018.06.017
Vasić, D., Ninkov, T., Bulatović, V., Sušić, Z. and Marković, M. (2014), "Terrain mapping by applying unmanned aerial vehicle and lidar system for the purpose of designing in Serbia", *Proceeding of the INGEO 2014-6th International Conference on Engineering Surveying*, Prague, Czech Republic.
Zhang, B., Wang, H., Huang, J. and Xu, N. (2019), "Model test on slope deformation and failure caused by transition from open-pit to underground mining", *Geomech. Eng.*, *Int. J.*, **19**(2), 167-178. https://doi.org/10.12989/gae.2019.19.2.167

HJ